Polymer Chemistry

ROYAL SOCIETY OF CHEMISTRY

PAPER

View Article Online
View Journal | View Issue

Cite this: *Polym. Chem.*, 2022, **13**, 2608

Depolymerizable semi-fluorinated polymers for sustainable functional materials†

Devavrat Sathe, ‡[a] Junfeng Zhou, ‡[a] Hanlin Chen,[a] Briana R. Schrage,[b] Seiyoung Yoon,[a] Zeyu Wang,[a] Christopher J. Ziegler[b] and Junpeng Wang *[a]

Fluorinated polymers are important functional materials for a broad range of applications, but the recycling of current fluorinated polymers is challenging. We present the first example of semi-fluorinated polymers that can undergo chemical recycling to form the corresponding monomers under ambient conditions. Prepared through ring-opening metathesis polymerization of functionalized *trans*-cyclobutane fused cyclooctene (*t*CBCO) monomers, these polymers show tunable glass transition temperatures (−2 °C to 88 °C), excellent thermal stability (decomposition onset temperatures >280 °C) and hydrophobicity (water contact angles >90°). The hydrophobicity of the semi-fluorinated polymers was further utilized in an amphiphilic diblock copolymer, which forms self-assembled micelles with a size of ~88 nm in an aqueous solution. Finally, through an efficient, regioselective *para*-fluoro-thiol substitution reaction, post-polymerization functionalization of a polymer with a pentafluorophenyl imide substituent was achieved. The ease of preparation, functionalization, and recycling, along with the diverse thermomechanical properties and demonstrated hydrophobicity make the *t*CBCO-based depolymerizable semi-fluorinated polymers promising candidates for sustainable functional materials that can offer a solution to a circular economy.

Received 22nd February 2022,
Accepted 4th April 2022

DOI: 10.1039/d2py00240j

rsc.li/polymers

Introduction

Since the invention of polychlorotrifluoroethylene and polytetrafluoroethylene in the 1930s,[1,2] fluorinated polymers have come to hold a position of importance in functional materials. The high strength and low polarizability of the C–F bond along with its intrinsic tendency to form weaker van der Waals interactions impart fluorinated polymers with unique and valuable properties,[3–5] including high hydrophobicity and a low coefficient of friction, as well as solvent, thermal, and chemical resistance. Benefited from these useful properties, fluorinated polymers have become indispensable in a diverse range of applications, including hydrophobic materials,[6] parts for use in chemically harsh conditions,[7] anti-fouling[8,9] and low-friction surfaces,[10,11] dielectrics[12,13] and separation membranes.[14] The hydrophobicity of fluorinated polymers and their incompatibility with non-fluorinated polymers have also attracted significant interests in the field of self-assembly.[15]

The high-volume production and use of fluorinated polymers need to be backed up by effective recycling to achieve sustainable utilization of natural resources and to reduce environmental impact. At present, most post-consumer fluorinated and semi-fluorinated polymer waste ends up in landfills. This has raised environmental concerns since accumulation of fluorinated polymer waste can lead to the release of highly persistent microplastics that can become a part of the food chain.[16,17] Current effort in recycling of fluorinated polymers has been focused on mechanical recycling, which requires extensive sorting and the addition of harsh chemicals, and the mechanical processing of the refined material typically leads to the reduction in molecular weight and the deterioration in mechanical properties.[18]

A promising route to ensuring a closed-loop life cycle for fluorinated polymers is chemical recycling to monomers (CRM).[19] Polytetrafluoroethylene can depolymerize to form its monomer through pyrolysis; however, its pyrolytic depolymerization results in a mixture of tetrafluoroethene and other fluorinated small molecules, and the process requires high temperatures (>650 °C) and thus large energy inputs.[20,21] In addition, the pyrolytic depolymerization method is not applicable across a wide range of fluorinated and semi-fluorinated

[a]*School of Polymer Science and Polymer Engineering, The University of Akron, Akron, Ohio 44325, USA. E-mail: jwang6@uakron.edu*
[b]*Department of Chemistry, The University of Akron, Akron, Ohio 44325, USA*
†Electronic supplementary information (ESI) available. CCDC 2151352. For ESI and crystallographic data in CIF or other electronic format see DOI: **https://doi.org/10.1039/d2py00240j**
‡These authors have contributed equally.

materials. It is therefore desirable to develop fluorinated or semi-fluorinated polymers that can be depolymerized under mild conditions while maintaining their high thermal stability.

Recently, CRM has been successfully demonstrated with several polymer systems based on ring-opening polymerization of cyclic monomers, including lactones,[22,23] β-thiolactones,[24,25] cyclic acetals,[26] and cyclic olefins.[27,28] Importantly, the ring-closing depolymerization of these systems typically requires a catalyst; without the catalyst, the polymers are in a kinetic trap.[29] The mechanism of catalytic depolymerization has enabled high thermal stability to be achieved when the catalyst is removed from the system. Meanwhile, CRM can occur under mild conditions by introducing an appropriate catalyst. Despite the developments, there is a lack of a robust CRM system that allows functionalization without significantly altering the thermodynamics.[30]

We recently reported a CRM system based on *trans*-cyclobutane fused cyclooctene (*t*CBCO) monomers (Fig. 1a).[31] Polymers with high molecular weights, high thermal stability (T_d > 370 °C), and hydrolytically stable backbones were obtained. The facile synthesis and functionalization of the *t*CBCO systems allows us to access polymers of a wide range of glass transition temperatures (T_g, from −30 °C to 100 °C) by varying the functional groups on the cyclobutane. The polymers can be depolymerized under mild conditions to form the *t*CBCO monomers in the presence of Grubbs 2nd-generation catalyst (G2). Another unique feature of this system is that the driving force for polymerization can be elevated by isomerizing the *cis*-cyclooctene to its *trans* form, allowing the polymerization to be conducted in dilute monomer concentrations (≥25 mM).[32] Herein, we leverage the versatility of the *t*CBCO system and report chemically recyclable semi-fluorinated polymers (Fig. 1b, **P1–P3**). The materials exhibit high thermal stability, hydrophobicity, and tunable thermomechanical properties. In addition, a *t*CBCO diblock copolymer that comprises a semi-fluorinated block and a block containing poly (ethylene glycol) (PEG) side chains was synthesized and its self-assembly was investigated. Finally, the post-functionalization of a pentafluorophenyl imide functionalized polymer **P2** was demonstrated, which can be utilized to further edit the system.

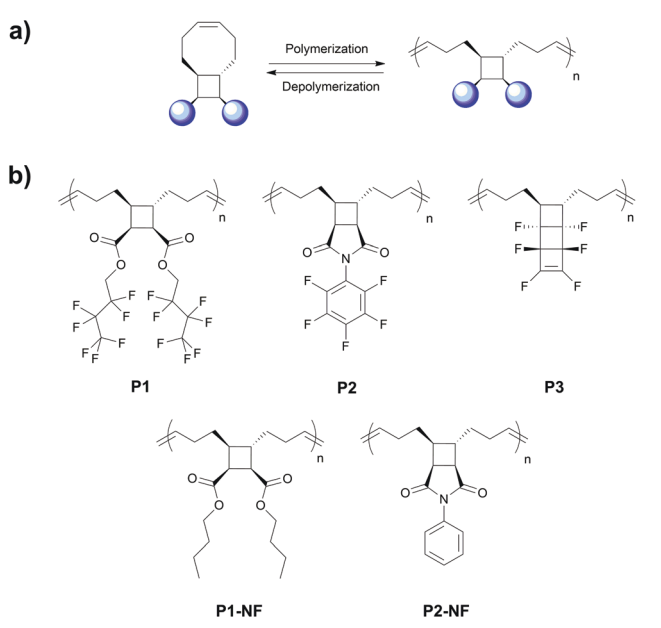

Fig. 1 Depolymerizable polymers based on *trans*-cyclobutane fused cyclooctene (*t*CBCO) monomers. (a) Installing a *trans*-cyclobutane ring on a 5,6-positions of cyclooctene renders the resulting ROMP polymer depolymerizable, and a diverse range of functional groups can be attached to the cyclobutane to tune the material properties of the polymer. (b) Semi-fluorinated polymers (**P1**, **P2**, and **P3**) and the non-fluorinated counterparts for **P1** (**P1-NF**) and **P2** (**P2-NF**) prepared and studied in this work.

Results and discussion

The synthetic scheme for the semi-fluorinated monomers used in this study **M1–M3** is shown in Fig. 2. A photochemical [2 + 2] cycloaddition of 1,5-cyclooctadiene (COD) and maleic anhydride led to **1**, which can undergo esterification with 2,2,3,3,4,4,4-heptafluoro-1-butanol to form **M1** or react with pentafluoroaniline to generate the imide **M2** (Fig. 2a). Monomer **M3** was prepared *via* a [2 + 2] photocycloaddition reaction between hexafluorobenzene and COD according to the method reported by Šket *et al.*[33] Contrary to their report that only *cis*-cylobutane products were detected, our studies suggest that both *cis*- and *trans*-cyclobutane fused isomers were obtained, with the *trans*-cyclobutane isomer being the major product (Fig. S1†). The predominant formation of *trans*-cyclobutane is consistent with the photocycloaddition of COD and maleic anhydride, suggesting isomerization prior to cycloaddition of the alkene in COD that forms cyclobutane.[34] Compared to the photocycloaddition of maleic anhydride with COD, which has a selectivity of *trans*/*cis* > 99/1, the lower selectivity for hexafluorobenzene (*trans*/*cis* = 93/7) could be attributed to a higher reactivity of hexafluorobenzene, according to the reactivity–selectivity principle.[35] The similar polarity of the *cis*- and *trans*-cyclobutane products renders separation by column chromatography inefficient. To facilitate the purification of **M3**, the mixture of isomers was subjected to ring-opening metathesis polymerization (ROMP) to form a polymer that contains both *cis*-and *trans*-cyclobutanes. According to our recent studies, the ring strain energy of the *trans*-cyclobutane fused cyclooctene is 5 kcal mol^{-1} lower than its *cis* analogue,[31] thus only the polymer of the *trans*-cyclobutane monomer can depolymerize to form the monomer. Indeed, subjecting the polymer that contains both isomers of cyclobutane to a depolymerization condition (1 mol% Grubbs 2nd-generation catalyst (G2), [olefin] = 0.1 M in $CHCl_3$, at 50 °C for 2 h) yielded a mixture of *trans*-cyclobutane isomer **M3** (without its *cis* analogue) and oligomers, from which **M3** was conveniently isolated. It is inconvenient to grow single crystal from **M3** since it is a liquid at room temperature; we therefore

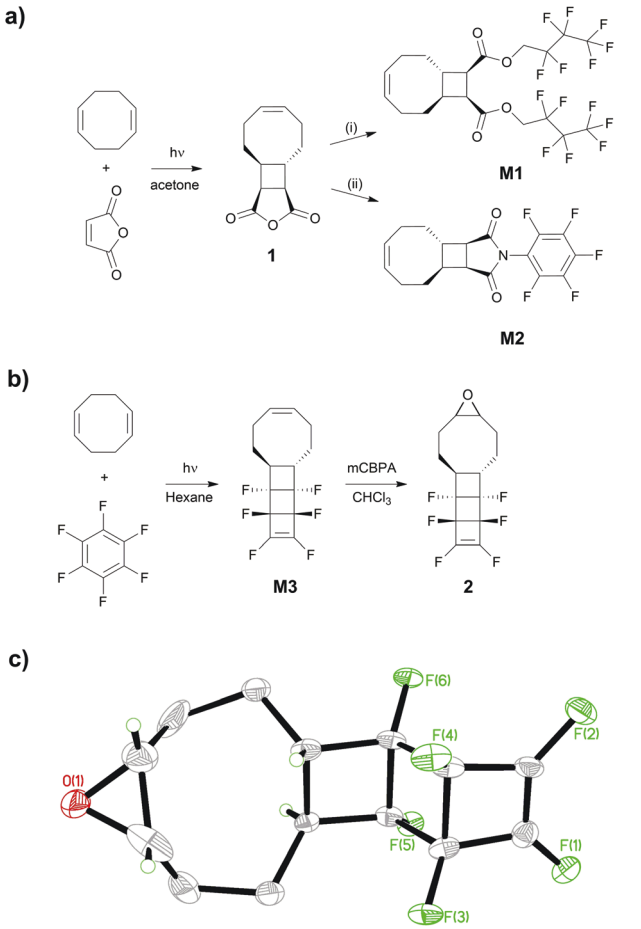

Fig. 2 Synthesis of *t*CBCO-based semi-fluorinated monomers. (a) Synthetic scheme for semi-fluorinated monomers **M1** and **M2**. Anhydride **1**, prepared through [2 + 2] photocycloaddition of 1,5-cyclooctadiene and maleic anhydride, is converted to **M1** and **M2** *via* conditions (i), and (ii), respectively. (i) MeOH, reflux; NaOH, H_2O, 60 °C; 2,2,3,3,4,4,4-heptafluoro-1-butanol, EDC, DMAP, DCM. (ii) Pentafluoroaniline, toluene, 90 °C; sodium acetate, acetic anhydride, 100 °C. (b) Synthetic scheme for **M3** and its epoxide **2**. (c) The structure of **2** with 35% thermal ellipsoids; methylene hydrogen atoms have been omitted for clarity.

Table 1 Molecular weight information and thermal properties of polymers listed in Fig. 1

Entry	M_n [a] (kDa)	$Đ$ [b]	T_d [c] (°C)	T_g [d] (°C)
P1	276	1.42	335	−2
P2	147	1.75	395	88
P3	108.3	1.64	298	13
P1-NF	66.9	3.74	370[e]	−31[e]
P2-NF	105.8	1.81	409[e]	100[e]

[a] M_n is the number average molecular weight measured using gel permeation chromatography (GPC) with THF as the eluent, calculated based on a polystyrene standard. [b] $Đ$ is the dispersity (M_w/M_n) determined by GPC. [c] T_d is the temperature at which the polymer experiences 5% weight loss as measured using thermogravimetric analysis. [d] T_g is the glass transition temperature as obtained using differential scanning calorimetry. [e] T_d and T_g for **P1-NF** and **P2-NF** are taken from ref. 31.

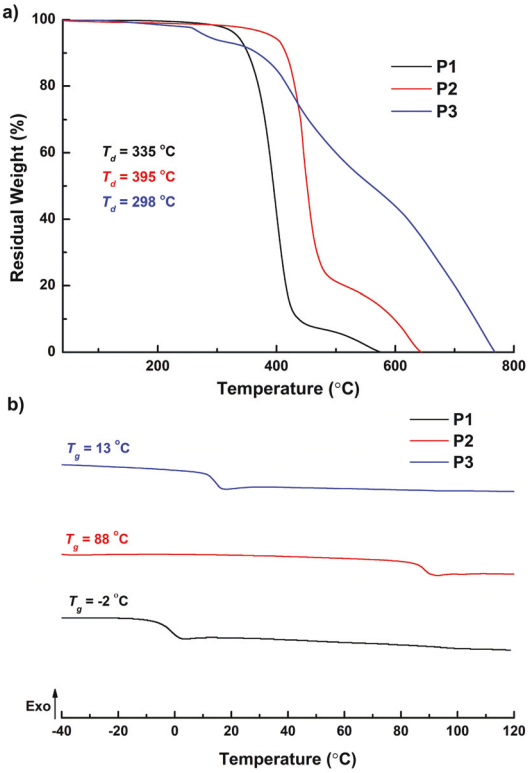

Fig. 3 Characterization of the thermal properties of the semi-fluorinated depolymerizable polymers **P1**, **P2**, and **P3**. (a) Thermogravimetric analysis. (b) Differential scanning calorimetry. T_g is the glass transition temperature while T_d is the temperature at which the polymer experiences 5% weight loss.

epoxidized it to obtain the compound **2**, which retains the stereochemistry of **M3** and is a solid at room temperature. The X-ray crystallography of the epoxide **2** (Fig. 2c, Table S2†) confirmed the *trans*-cyclobutane moiety in **M3.**

Monomers **M1**, **M2**, and **M3** were polymerized in the presence of G2 at monomer concentrations of >2 M at room temperature. High molecular weight polymers (M_n > 100 kDa) were obtained with broad dispersity ($Đ$ > 1.4) (Table 1). The relatively high dispersity values obtained here were also observed in the ROMP of other low strain monomers using G2.[36,37] The thermal properties of polymers **P1**, **P2** and **P3** were evaluated *via* thermogravimetric analysis (TGA) and differential scanning calorimetry (DSC). The TGA results (Fig. 3a and Table 1) showed that **P1** and **P2** have high thermal stability with T_d = 335 °C and 395 °C respectively; **P3**, however, showed a much broader, multi-step thermal decomposition with a lower decomposition temperature of 298 °C. The DSC curves (Fig. 3b, Fig. S42,† and Table 1) revealed that all three polymers are amorphous, as each polymer showed only a glass transition temperature (T_g) with no melting temperature. The polymers exhibited a wide range of T_gs: **P1** with the more flexible heptafluorobutyl ester side chains showed the lowest T_g of −2 °C while the highest T_g (88 °C) was observed for **P2**, which

possesses a rigid pentafluorophenyl imide substituent. **P3**, which contains a fluorinated ladderane[38] had a moderate T_g of ~13 °C. Additionally, the DSC curve of **P3** showed a large exothermic peak with an onset at ~155 °C, possibly due to side reactions that cause crosslinking (see extended DSC traces in Fig. S42†). Compared to its non-fluorinated counterpart **P1-NF**, which has a T_g of about −31 °C,[31] **P1** showed a ~29 °C increase in T_g; a similar effect has been previously observed in the comparison between poly(butyl acrylate) and poly(2,2,3,3,4,4,4-heptafluorobutyl acrylate), the T_gs of which are −50 °C and −18 °C, respectively.[39] Interestingly, **P2** showed the opposite behaviour compared to **P2-NF**, with a decrease in T_g of ~12 °C. This is similar to what has been observed for ROMP polymers of *N*-pentafluorophenyl norbornene-5,6-carboximide (T_g = 171 °C) as compared to its non-fluorinated counterpart (T_g = 222 °C), albeit to a lesser magnitude.[40] The wide-range of thermal properties obtained herein again highlight the ease with which the thermomechanical properties of the *t*CBCO polymers can be tuned by simply varying the functional groups attached to cyclobutane.

The depolymerization of **P1**, **P2** and **P3** were studied at a range of concentrations ($[olefin]_0$ = 25 mM, 50 mM, 100 mM, 200 mM, and 400 mM). The polymer solutions in chloroform were stirred with 1 mol% or 2 mol% G2 at room temperature for ~16 h, which according to our previous kinetic studies, is sufficient for the depolymerization to reach the thermodynamic equilibrium.[31] GPC traces of the depolymerized polymers showed the disappearance of the polymer peak and the appearance of a new peak corresponding to the monomer at longer retention times, along with a small broad peak corresponding to a small amount of residual cyclic oligomers (Fig. S2†). The extent of depolymerization was calculated by integrating the peaks corresponding to the olefinic protons that correspond to the monomers and the polymer/oligomers in the ^{1}H NMR spectra (Fig. S3–S5†). At [olefin] ≤ 50 mM, **P1**, **P2** and **P3** all reached at least 90% depolymerization (Fig. 4). At higher concentrations, the extent of depolymerization showed a trend of **P1** > **P3** > **P2**. For example, at [olefin] = 400 mM, **P1** could be depolymerized to 87% while **P2** and **P3** to 34% and 61%, respectively. These observations are in agreement with our previous observation that an additional fused ring attached to the cyclobutane can raise the ceiling temperature and inhibit depolymerization[31] and demonstrate the possibility of tuning the thermodynamics of depolymerization through substituent effect.[41]

To evaluate the hydrophobicity of the semi-fluorinated polymers, films of **P1**, **P2**, and **P3** were prepared on glass slides and their static water contact angles were measured. Both **P1** (97.4°) and **P2** (91.6°) showed higher contact angles than their non-fluorinated counterparts **P1-NF** (89.7°) and **P2-NF** (73.1°), respectively (Fig. 5). All three semi-fluorinated polymers **P1**, **P2** and **P3** showed hydrophobicity with contact angles over 90° (Fig. 5), with **P1** having the highest contact angle (97.4°), followed by **P3** (94.7°) and **P2** (91.6°). This trend is consistent with the fluorine content in these polymers: 45 wt% in **P1**, 26 wt% in **P2** and 39 wt% in **P3**. Previous studies involving angle-resolved X-ray photoelectron spectroscopy (XPS) of polymers with semi-fluorinated side chains showed that fluorinated side chains preferentially orient towards the polymer surface, thus resulting in higher fluorine content at the polymer surface than in the bulk.[42,43] The preferential orientation of fluorinated groups at the surface positively correlated with the mass fraction of fluorine;[42] fluorine content as a fraction of total surface atoms was also shown to increase with the total mass fraction of fluorine atoms in the polymer, which is correlated with the water contact angle of the polymer.[43] It is likely that such surface orientation effects also contribute to the trend in water contact angles that we see here.

Having established the hydrophobicity of our semi-fluorinated polymers, we decided to exploit this behaviour in an

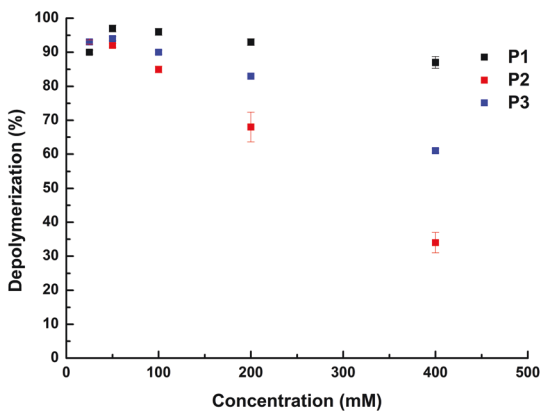

Fig. 4 The extent of depolymerization obtained at various concentrations for the semi-fluorinated depolymerizable polymers **P1**, **P2** and **P3**. Reaction time: 16 h.

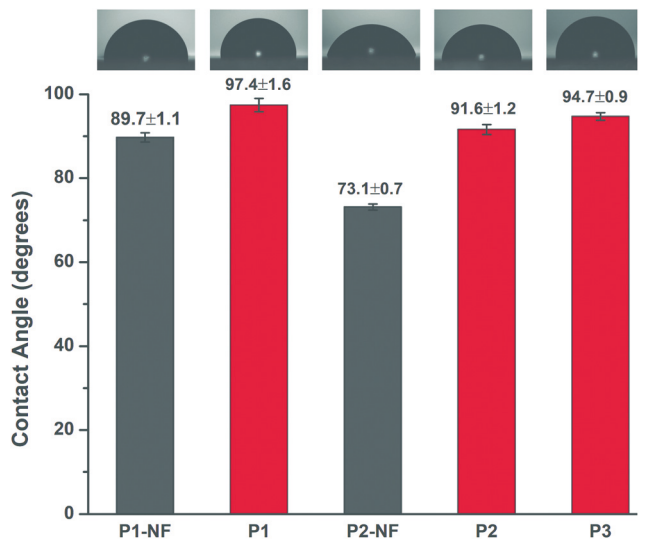

Fig. 5 Water contact angles for the semi-fluorinated depolymerizable polymers **P1**, **P2**, and **P3**, and for non-fluorinated polymers **P1-NF** and **P2-NF**.

amphiphilic block copolymer. We leveraged the living ROMP of *trans*-cyclooctene and prepared a diblock copolymer **P1-*b*-P4**, by sequentially polymerizing ***E*-M1** and a PEG functionalized monomer ***E*-M4** (see ESI†). We hypothesized that the presence of two incompatible blocks, *i.e.*, a hydrophobic fluorinated block and a hydrophilic PEG block, would enable the self-assembly of the block copolymer into micellar structures in an appropriate solvent. To evaluate the solution self-assembly of **P1-*b*-P4**, the polymer was first dissolved in THF at a concentration of 10 mg mL^{-1}, and to this solution deionized water was slowly added, similar to the method described by Discekici *et al.*[44] Dynamic light scattering measurement of the aqueous solution showed a particle size of ~88 nm with polydispersity of 0.279 (Fig. 6), indicating the successful self-assembly of the block copolymer into a micellar structure.

Finally, aiming to further enhance the versatility of the polymer system, we explored post-polymerization functionalization of the pentafluorophenyl imide functionalized polymer **P2**. This was achieved through a nucleophilic aromatic substitution (S_NAr) of the *para*-fluoro atom in the pentafluorophenyl unit with an aromatic thiol. The mild conditions, quantitative conversion, and regiospecific substitution at the *para*-fluoro position together make this reaction particularly useful for post-polymerization functionalization.[45] Thiophenol (1.05 eq. with respect to the *p*-fluoro atoms in **P2**) was employed as the nucleophile while an excess of K_2CO_3 (1.5 eq.) was added as the base, and the reaction was carried out in 2-butanone at 80 °C. Quantitative substitution of the *para*-fluoro atoms and formation of **P2-SPh** was observed from the ^{19}F NMR spectra (Fig. 7a), indicated by the disappearance of the peak corresponding to the *para*-fluoro atom in **P2** at −152.12 ppm and a downfield shift of the *m*-fluoro peak from **P2** to **P2-SPh** by ~29 ppm. The GPC traces (Fig. 7c) did not show any significant changes in the molecular weight distribution, while only a slight increase in the molecular weight was observed (M_n measured to be 98.6 kDa for **P2** and 103.2 kDa for **P2-SPh**). Note that the measured molecular weight for **P2-SPh** is lower than the expected molecular weight (122.6 kDa) assuming 100% substitution. Since the molecular weights reported here were obtained by measuring the hydrodynamic sizes and comparing them to a polystyrene standard, it is likely that the substitution reaction only slightly increased the hydrodynamic radius of **P2** despite increasing its actual molecular weight by ~24.3%. As a result, only a minor change in M_n was observed. These effects on the molecular weight and dispersity are similar to those observed for the substitution of poly(2,3,4,5,6-pentafluorobenzyl acrylate) with thiophenol by Noy *et al.*[46]

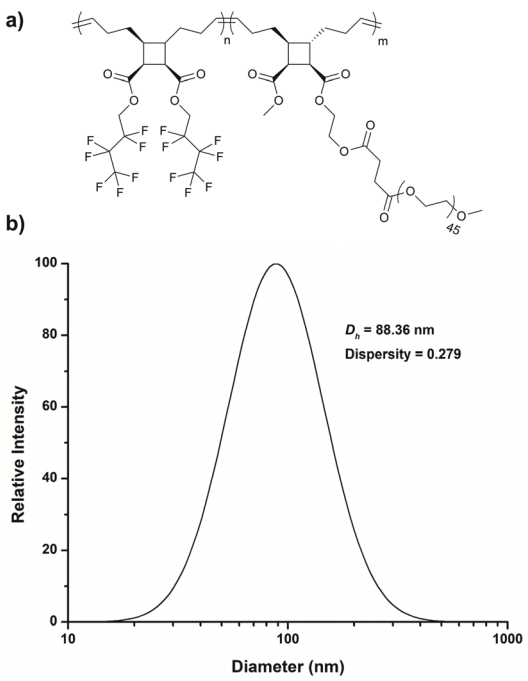

Fig. 6 Self-assembly of block copolymer **P1-*b*-P4**. (a) Structure and (b) dynamic light scattering spectrum for block copolymer **P1-*b*-P4**.

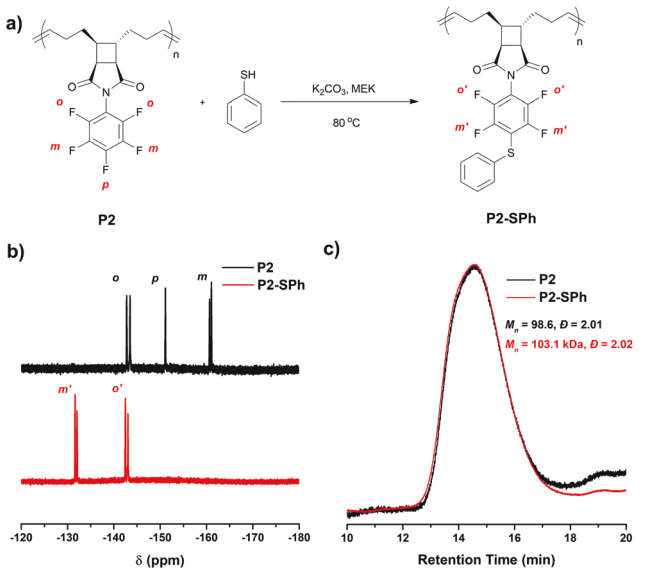

Fig. 7 Post-polymerization functionalization of **P2** *via para*-fluoro thiol ligation. (a) Synthetic scheme for the nucleophilic aromatic substitution of thiophenol on **P2**. ^{19}F NMR spectra (b) and GPC traces (c) for **P2** before and after functionalization (M_n was calculated based on polystyrene standards).

Conclusions

Fluorinated polymers pose a significant challenge to closed-loop recycling: most post-consumer fluorinated polymer waste ends up in landfills, while the persistence of these materials along with the hazards caused by fluorinated small molecules has led to rising concerns about the disposal of such waste.[16,47,48] We have introduced the first example of semi-fluorinated polymers that can undergo CRM under ambient conditions. The polymers shown here can be depolymerized to over 90% conversion in the presence of ruthenium-based catalysts at room temperature while the modular nature of the

*t*CBCO scaffold has been utilized to incorporate diverse thermomechanical properties. The materials show hydrophobicity, with water contact angles as high as 97.4°, and the hydrophobicity has been further exploited as an amphiphilic diblock copolymer that can form self-assembled micellar structures. The depolymerizable amphiphilic polymers demonstrated here can be used in applications such as antifouling materials[49,50] and controlled small-molecule release.[51,52] Finally, we have also demonstrated facile post-polymerization functionalization of a pentafluorophenyl imide functionalized polymer as a strategy to introduce an additional degree of versatility and functionality, which can be used to prepare complex polymer topologies including star polymers,[53] graft copolymers,[54] and polymer networks.[55] Through the materials developed here, we have expanded the concept of CRM into the domain of fluorinated materials, where such developments were limited to highly energy intensive processes and a small number of materials. We envision that the versatility of this system will enable further incorporation of chemical recyclable polymers into areas where it has been hitherto lacking, including elastomers, thermosets, and fibre-reinforced polymer composites.

Author contributions

D.S, J.Z., and J.W. conceived and designed the experiments. D.S., J.Z., H.C., S.Y., and Z.W. performed the synthesis. B.R.S. and C.J.Z. collected and analysed the single-crystal data. D.S. and J.Z. conducted the thermal characterization, depolymerization studies and contact angle measurements. D.S. conducted the DLS measurement and post-polymerization functionalization studies. D.S., J.Z., and J.W. wrote the manuscript.

Conflicts of interest

There are no conflicts of interest to declare.

Acknowledgements

This material is based on work supported by the University of Akron and the National Science Foundation under grant DMR-2042494. The single-crystal structures were characterized with an X-ray diffractometer supported by the National Science Foundation (CHE-0840446 to C. J. Z.).

References

1 Q.-D. Shen, in *Dielectric Polymer Materials for High-Density Energy Storage*, ed. Z.-M. Dang, William Andrew Publishing, Cambridge, 2018, ch. 3, pp. 59–102.
2 R. J. Plunkett, *US Pat.*, 2230654A, 1941.
3 D. O'Hagan, *Chem. Soc. Rev.*, 2008, **37**, 308–319.
4 V. H. Dalvi and P. J. Rossky, *Proc. Natl. Acad. Sci. U. S. A.*, 2010, **107**, 13603–13607.
5 R. R. Thomas, in *Fluoropolymers 2*, ed. P. E. Cassidy, K. Johns and T. Davidson, Springer, Boston, 2 edn, 2006, ch. 4, pp. 47–67.
6 C. R. Crick and I. P. Parkin, *Chem. – Eur. J.*, 2010, **16**, 3568–3588.
7 P. R. Khaladkar and S. Ebnesajjad, *Fluoropolymer applications in the Chemical Processing Industries: The definitive user's guide and handbook*, William Andrew Publishing, Cambridge, 2018.
8 X. Sun, C. Wu, J. Hu, X. Huang, G. Lu and C. Feng, *Langmuir*, 2019, **35**, 1235–1241.
9 W. Van Zoelen, H. G. Buss, N. C. Ellebracht, N. A. Lynd, D. A. Fischer, J. Finlay, S. Hill, M. E. Callow, J. A. Callow, E. J. Kramer, R. N. Zuckermann and R. A. Segalman, *ACS Macro Lett.*, 2014, **3**, 364–368.
10 N. S. Bhairamadgi, S. P. Pujari, F. A. M. Leermakers, C. J. M. Van Rijn and H. Zuilhof, *Langmuir*, 2014, **30**, 2068–2076.
11 N. S. Bhairamadgi, S. P. Pujari, C. J. M. Van Rijn and H. Zuilhof, *Langmuir*, 2014, **30**, 12532–12540.
12 W. Volksen, R. D. Miller and G. Dubois, *Chem. Rev.*, 2010, **110**, 56–110.
13 Prateek, V. K. Thakur and R. K. Gupta, *Chem. Rev.*, 2016, **116**, 4260–4317.
14 Z. Cui, E. Drioli and Y. M. Lee, *Prog. Polym. Sci.*, 2014, **39**, 164–198.
15 M. Guerre, G. Lopez, B. Améduri, M. Semsarilar and V. Ladmiral, *Polym. Chem.*, 2021, **12**, 3852–3877.
16 R. Lohmann, I. T. Cousins, J. C. Dewitt, J. Glüge, G. Goldenman, D. Herzke, A. B. Lindstrom, M. F. Miller, C. A. Ng, S. Patton, M. Scheringer, X. Trier and Z. Wang, *Environ. Sci. Technol.*, 2020, **54**, 12820–12828.
17 M. Geiser, S. Schürch and P. Gehr, *J. Appl. Physiol.*, 2003, **94**, 1793–1801.
18 S. Ebnesajjad, in *Introduction to Fluoropolymers: Materials, Technology and Applications*, ed. S. Ebnesajjad, William Andrew Publishing, Waltham, 2013, ch. 13, pp. 293–309.
19 G. W. Coates and Y. D. Y. L. Getzler, *Nat. Rev. Mater.*, 2020, **5**, 501–516.
20 E. E. Lewis and M. A. Naylor, *J. Am. Chem. Soc.*, 1947, **69**, 1968–1970.
21 K. Hintzer and W. Schwertfeger, in *Handbook of Fluoropolymer Science and Technology*, ed. D. W. Smith, S. T. Iacono and S. S. Iyer, John Wiley & Sons, Inc., Hoboken, 2014, ch. 21, pp. 495–520.
22 J. B. Zhu, E. M. Watson, J. Tang and E. Y. X. Chen, *Science*, 2018, **360**, 398–403.
23 M. Hong and E. Y. X. Chen, *Nat. Chem.*, 2016, **8**, 42–49.
24 J. Yuan, W. Xiong, X. Zhou, Y. Zhang, D. Shi, Z. Li and H. Lu, *J. Am. Chem. Soc.*, 2019, **141**, 4928–4935.
25 W. Xiong, W. Chang, D. Shi, L. Yang, Z. Tian, H. Wang, Z. Zhang, X. Zhou, E. Q. Chen and H. Lu, *Chem*, 2020, **6**, 1831–1843.

26 B. A. Abel, R. L. Snyder and G. W. Coates, *Science*, 2021, **373**, 783–789.
27 J. D. Feist and Y. Xia, *J. Am. Chem. Soc.*, 2020, **142**, 1186–1189.
28 W. J. Neary, T. A. Isais and J. G. Kennemur, *J. Am. Chem. Soc.*, 2019, **141**, 14220–14229.
29 C. Shi, L. T. Reilly, V. S. Phani Kumar, M. W. Coile, S. R. Nicholson, L. J. Broadbelt, G. T. Beckham and E. Y. X. Chen, *Chem*, 2021, **7**, 2896–2912.
30 W. J. Neary and J. G. Kennemur, *ACS Macro Lett.*, 2019, **8**, 46–56.
31 D. Sathe, J. Zhou, H. Chen, H.-W. Su, W. Xie, T.-G. Hsu, B. R. Schrage, T. Smith, C. J. Ziegler and J. Wang, *Nat. Chem.*, 2021, **13**, 743–750.
32 H. Chen, Z. Shi, T. G. Hsu and J. Wang, *Angew. Chem., Int. Ed.*, 2021, **60**, 25493–25498.
33 B. Šket, N. Zupančič and M. Zupan, *J. Chem. Soc., Perkin Trans. 1*, 1987, 981–985.
34 T.-G. Hsu, J. Zhou, H.-W. Su, B. R. Schrage, C. J. Ziegler and J. Wang, *J. Am. Chem. Soc.*, 2020, **142**, 2100–2104.
35 E. V. Anslyn and D. A. Dougherty, *Modern Physical Organic Chemistry*, University Science Books, Sausalito, 2005.
36 A. Hejl, O. A. Scherman and R. H. Grubbs, *Macromolecules*, 2005, **38**, 7214–7218.
37 A. R. Hlil, J. Balogh, S. Moncho, H.-L. Su, R. Tuba, E. N. Brothers, M. Al-Hashimi and H. S. Bazzi, *J. Polym. Sci., Part A: Polym. Chem.*, 2017, **55**, 3137–3145.
38 B. R. Boswell, C. M. F. Mansson, J. M. Cox, Z. Jin, J. A. H. Romaniuk, K. P. Lindquist, L. Cegelski, Y. Xia, S. A. Lopez and N. Z. Burns, *Nat. Chem.*, 2021, **13**, 41–46.
39 B. P. Koiry, H. A. Klok and N. K. Singha, *J. Fluorine Chem.*, 2014, **165**, 109–115.
40 A. A. Santiago, J. Vargas, S. Fomine, R. Gaviño and M. A. Tlenkopatchev, *J. Polym. Sci., Part A: Polym. Chem.*, 2010, **48**, 2925–2933.
41 J. Zhou, D. Sathe and J. Wang, *J. Am. Chem. Soc.*, 2022, **144**, 928–934.
42 G. Beamson and M. R. Alexander, *Surf. Interface Anal.*, 2004, **36**, 323–333.
43 R. D. Van de Grampel, W. Ming, A. Gildenpfennig, W. J. H. Van Gennip, M. J. Krupers, J. Laven, J. W. Niemantsverdriet, H. H. Brongersma and R. R. Van der Linde, *Prog. Org. Coat.*, 2002, **45**, 273–279.
44 E. H. Discekici, A. Anastasaki, R. Kaminker, J. Willenbacher, N. P. Truong, C. Fleischmann, B. Oschmann, D. J. Lunn, J. Read De Alaniz, T. P. Davis, C. M. Bates and C. J. Hawker, *J. Am. Chem. Soc.*, 2017, **139**, 5939–5945.
45 S. Agar, E. Baysak, G. Hizal, U. Tunca and H. Durmaz, *J. Polym. Sci., Part A: Polym. Chem.*, 2018, **56**, 1181–1198.
46 J. M. Noy, A. K. Friedrich, K. Batten, M. N. Bhebhe, N. Busatto, R. R. Batchelor, A. Kristanti, Y. Pei and P. J. Roth, *Macromolecules*, 2017, **50**, 7028–7040.
47 M. H. Russell, W. R. Berti, S. Bogdan and R. C. Buck, *Environ. Sci. Technol.*, 2007, **42**, 800–807.
48 M. H. Russell, W. R. Berti, B. Szostek, N. Wang and R. C. Buck, *Polym. Degrad. Stab.*, 2010, **95**, 79–85.
49 J. Xu, D. A. Bohnsack, M. E. Mackay and K. L. Wooley, *J. Am. Chem. Soc.*, 2007, **129**, 506–507.
50 H. Guo, P. Chen, S. Tian, Y. Ma, Q. Li, C. Wen, J. Yang and L. Zhang, *Langmuir*, 2020, **36**, 14573–14581.
51 J. Park, S. Jo, Y. M. Lee, G. Saravanakumar, J. Lee, D. Park and W. J. Kim, *ACS Appl. Mater. Interfaces*, 2021, **13**, 8060–8070.
52 B. Fan and E. R. Gillies, *Mol. Pharm.*, 2017, **14**, 2548–2559.
53 N. Cakir, U. Tunca, G. Hizal and H. Durmaz, *Macromol. Chem. Phys.*, 2016, **217**, 636–645.
54 T. Cai, W. J. Yang, K. Neoh and E. Kang, *Polym. Chem.*, 2012, **3**, 1061–1068.
55 F. Cavalli, H. Mutlu, S. O. Steinmueller and L. Barner, *Polym. Chem.*, 2017, **8**, 3778–3782.